ACS OMEGA
Open Access

http://pubs.acs.org/journal/acsodf
Article

Facile Synthesis of Nanostructured Lithium-Incorporated Titanium Oxides (Li-TiO$_x$) by Means of Wet Corrosion Process (WCP) and Their Potential Application for Batteries

Hiroto Suzuki, Takumi Nishiguchi, Yuta Igawa, Hiroya Oshiumi, Ki-Young Lee, Sanghoon Kim, Eunji Im, Siha Lee, Haneul Kim, Hatsuko Yoshikubo, Hazime Kiyono, and So Yoon Lee*

Cite This: *ACS Omega* 2025, 10, 207–214

ABSTRACT: Currently, there is a growing demand for nanomaterials in the fields of materials and energy. Nanostructured metal oxides have been widely studied, owing to their unique and diverse physicochemical properties and potential applications in various fields. In recent years, considerable attention has been directed toward metal oxides, particularly lithium-incorporated titanium oxides (Li-TiO$_x$), owing to their exceptional safety profiles. This material has been used in automotive battery systems, which has prompted extensive research efforts to enhance its functional properties. In response to the demand for superior nanomaterials, this study attempts to fabricate nanostructured Li-TiO$_x$ using a wet corrosion process (WCP). WCP refers to a novel method for fabricating nanostructures that employ alkaline solutions. This technique offers numerous advantages, such as short processing times, high reproducibility, and low cost. As a result of experiments, nanostructured Li-TiO$_x$ were successfully fabricated using LiOH solutions ranging in concentration from 0.5 to 2 mol/L. The fabricated nanostructures exhibited superior characteristic properties, such as increased surface area and enhanced electrical properties, when compared with those of untreated titanium. This study demonstrates that WCP is a simple, versatile, and scalable method for producing nanostructured Li-TiO$_x$ tailored for battery applications.

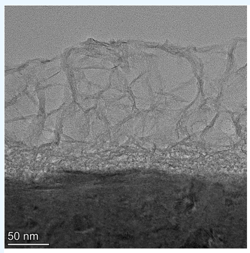

Nanostructured Li-TiO$_x$ fabricated via WCP

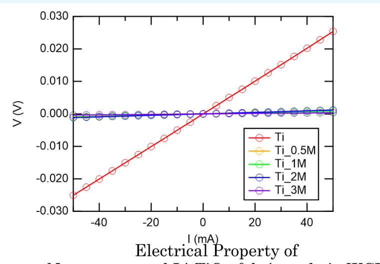

Electrical Property of Nanostructured Li-TiO$_x$ fabricated via WCP

1. INTRODUCTION

Nanostructured materials, defined as those with dimensions smaller than 100 nm, have been extensively studied because of their diverse physicochemical properties and potential for various applications owing to their size.[1−4] Hence, nanostructured materials are expected to bring about significant transformations in a wide range of fields, including electronics, mechanics, energy/environment, biotechnology, and pharmaceuticals.[5] In recent years, Ti-based materials have garnered significant attention in fields such as solar cells and biosensors owing to their multifunctional semiconductor properties, photocatalytic properties, and high dielectric constants. Nanostructured titanium materials have been extensively studied in various fields because of their chemical and biological inertness, photostability, and low cost.[6−9] Figure 1 shows the diverse applications of titanium oxides.

Nanostructured metal oxides have been extensively studied over the past few decades because of their unique and diverse physicochemical properties and a wide range of potential applications.[10] Nanostructured alkali metal-incorporated titanates containing A—Ti-O (A = alkali element and/or H) bonds have attracted considerable interest because of their unique layered structure.[11−15] The presence of alkali metal atoms in these titanates can significantly influence their physical properties; thus, research has been conducted across various fields, such as electric devices, photocatalysts, energy storage, and sensors, to adjust their physical properties.[10,16] Among titanium oxides containing alkali metals, Li-incorporated titanium oxides (Li-TiO$_x$), the focus of this study, have garnered attention in the field of energy devices.[16] Li-TiO$_x$ containing Li^+ ions are expected to be used in automotive batteries because of their excellent safety, prompting extensive research aimed at enhancing their functionality. However, a limitation of Li-ion batteries utilizing Li-TiO$_x$ is their relatively small battery capacity, which is a primary concern. One method that has been proposed to address this issue is the fabrication of nanostructures. The fabrication of Li-TiO$_x$ with nanostructures is currently one of the key issues in this

Received: May 16, 2024
Revised: November 21, 2024
Accepted: November 28, 2024
Published: December 19, 2024

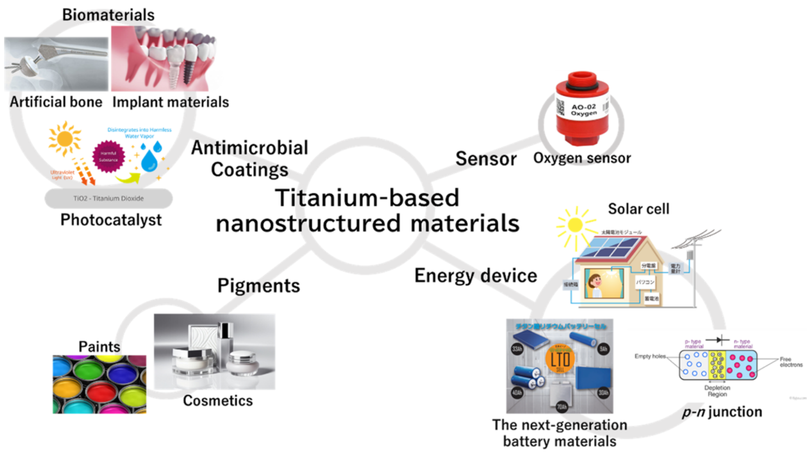

Figure 1. Schematic diagram of applications of titanium-based nanostructured materials in real life.

research field because it is expected to enhance the reactivity owing to the increased surface area resulting from nanostructures. Although nanostructured Li-TiO_x films are one of the leaders in this new class of materials, their synthesis still has limitations. Although several synthesis methods such as the sol−gel process, template-mediated process, and hydrothermal route have been developed to obtain the desired structural, chemical, and physical properties, nanostructure fabrication generally involves complicated processes, low reproducibility, and high costs for well-controlled chemical modification.[14−28] Furthermore, nanostructured titanium oxide films containing alkaline ions may be significantly influenced by the size and morphology of the nanostructures, as well as the concentration of the incorporated alkaline ions. Therefore, it may be necessary to combine multiple processes, and the aforementioned drawbacks may become even more pronounced.[10] To address these challenges, new techniques for fabricating nanostructures are required. In this study, we focus on a novel technique called the wet corrosion process (WCP) to fabricate nanostructured Li-TiO_x.

WCP uses alkaline solutions (e.g., NaOH and KOH) to corrode metals and fabricate nanostructures on their surfaces. WCP has many advantages, such as room-temperature processing, no heat treatment, short processing time, high reproducibility, and low cost, and has attracted much attention in the field of materials engineering. The nanostructures fabricated via WCP incorporated alkaline ions (Na^+, K^+) from the alkaline solution, thereby exhibiting electrical properties. Consequently, these electrical properties can be harnessed to utilize nanostructures in various functional materials.

In this study, we fabricated nanostructures on a pure Ti surface using WCP and determined the relationship between the morphology of the nanostructures and the WCP conditions. Furthermore, we investigated the potential for fabricating nanostructured Li-TiO_x using WCP with a LiOH solution, elucidated the fabrication conditions for nanostructures, and subsequently explored their application in batteries with the aim of contributing to global research efforts.

2. EXPERIMENTAL METHODS AND CHARACTERIZATIONS

2.1. Preparation of Alkaline Solution for WCP. Approximately 5.99 g of lithium hydroxide (Sigma-Aldrich Co., Ltd., Tokyo, Japan) was weighed using an electronic balance, and 50 mL of pure water was placed in a 500 mL polypropylene beaker for dissolution. Thereafter, a magnetic stirrer bar and stir place were used to continue stirring until the temperature of the solution decreased. The prepared LiOH solution was transferred to a 500 mL light-shielding bottle and stored in the dark.

2.2. Preparation of Nanostructured Li-TiO_x. Commercially available pure Ti substrates (>99%) were used in this study. All metal substrates, 10 mm × 10 × 1.0 mm^3 in size (light image), were polished with #400−#2000 SiC paper and washed with pure acetone and distilled water in an ultrasonic cleaner. Then, alkali treatment was performed by soaking all of these substrates in 5 mL of LiOH aqueous solutions with various concentrations from 0.1 to 5 mol/L at room temperature for 24 h. The prepared Ti substrates were placed in a tube containing a LiOH solution, and the upper part of the tube was covered with paraffin. After the alkali treatment, all metal substrates were gently washed with distilled water.

2.3. Characterizations. The changes in the surface morphology (structure, shape, and size) of the obtained samples were observed using field-emission scanning electron microscopy (FE-SEM) (JSM-7610F, Jeol Ltd., Tokyo, Japan) at 15 kV. Transmission electron microscopy (TEM) was used to observe the microstructure, and energy-dispersive X-ray spectroscopy (EDS) equipped with TEM was used to observe the elements on the surface. Atomic force microscopy (AFM) was used to observe the surface structure and specific surface area. X-ray photoelectron spectroscopy (XPS) was used to investigate the elemental composition and chemical bonding state of the fabricated nanostructured lithium titanium oxide. To investigate the electrical properties of samples, a current meter (Keithley) 6221 and a voltmeter (Keithley) 2182 were used.

3. RESULTS AND DISCUSSION

3.1. Synthesizing of the Nanostructures on the Ti Substrate after WCP. Figure 2 shows FE-SEM images of the surfaces of the obtained Ti substrates treated with 0.1, 0.5, 1, 2, 3, 4, and 5 mol/L LiOH solution at room temperature for 24 h.

Nanostructured titanium oxide was successfully fabricated on the surface of Ti treated with LiOH solutions at concentrations of 0.5, 1, and 2 mol/L. However, nanostructures were not observed on the surface of the Ti treated with LiOH solutions at concentrations of 0.1 mol/L and above 3 mol/L. This is believed to be because, when the LiOH solution

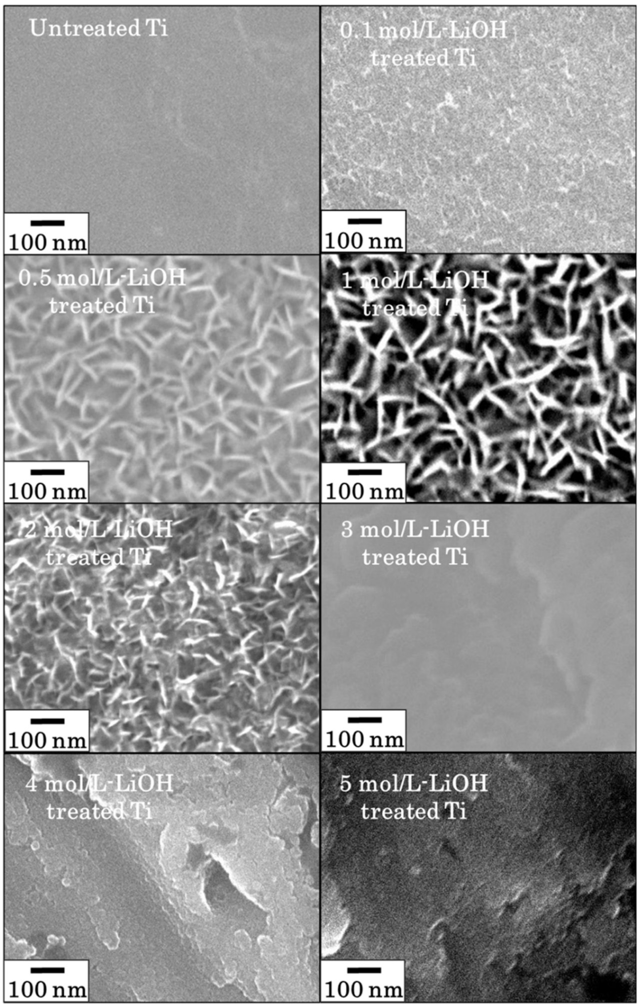

Figure 2. Top view scanning electron microscopy (SEM) images of untreated Ti and Ti surfaces treated with LiOH solutions at various concentrations.

concentration is low, the etching ability of the LiOH solution is weak and it cannot sufficiently react with the Ti surface. However, when the LiOH solution concentration was too high, the Ti surface reacted excessively with the LiOH solution, inhibiting the formation of the nanostructures. Therefore, based on the SEM results, it was confirmed that the minimum LiOH solution concentration capable of fabricating nanostructures is 0.5 mol/L, and the maximum concentration is 2 mol/L. Additionally, when performing WCP treatment using a LiOH solution, it is considered that the shape of the fabricated nanostructures does not depend on the solution concentration.

Nanostructured titanium oxide obtained by WCP was fabricated through partial dissolution of the Ti substrate by the LiOH solution, forming Ti−O bonds. The chemical reactions that occur during this process are represented by eqs 1−5.[10]

$$TiO_2 + OH^- = HTiO_3^- \tag{1}$$

$$Ti + 3OH^- = Ti(OH)_3^+ + 4e^- \tag{2}$$

$$Ti(OH)_3^+ + e^- = TiO_2{\cdot}H_2O + 1/2H_2 \tag{3}$$

$$Ti(OH)_3^+ + OH^- = Ti(OH)_4 \tag{4}$$

$$TiO_2{\cdot}nH_2O + OH^- = HTiO_3^-{\cdot}nH_2O \tag{5}$$

Nanostructures fabricated with 1 and 2 mol/L LiOH solutions exhibited no differences in shape. Therefore, the sample treated with the lower concentration of a 1 mol/L LiOH solution was selected as the representative sample for subsequent measurements.

Figure 3 shows the SEM images of the edge of untreated Ti and Ti treated with a 1 mol/L LiOH solution. It was confirmed that the nanostructures could be uniformly fabricated on the Ti surface using WCP.

3.2. Observation of the Synthesized Microstructures after WCP. Figure 4 illustrates the cross-sectional TEM images of the untreated Ti and Ti treated with 0.5 and 1 mol/L LiOH solutions.

From Figure 5, it was confirmed that the fabricated nanostructures were wire-like with a diameter of 5−10 nm for the nanowires. Additionally, the thicknesses of the layers of the nanostructures fabricated using 0.5 and 1 mol/L LiOH solutions were 120 and 200 nm, respectively. Furthermore, based on the TEM results, it is possible to discuss the generation mechanism of the nanostructures in the WCP. A schematic of the generation mechanism of the nanostructures is shown in Figure 5.

Figure 6 shows the TEM images of the nanostructured titanium oxide fabricated by using a 1 mol/L LiOH solution.

As shown in Figure 6, the lattice spacing of the fabricated nanostructured titanium oxide is 0.48 nm. This value closely matches the $d(111)$ lattice spacing of $Li_4Ti_5O_{12}$, suggesting that the fabricated nanostructured titanium oxide had a composition similar to $Li_4Ti_5O_{12}$.[29] This hypothesis is very impactful because it can be considered that the obtained products are Li-TiO_x. This indicates that our experiments aimed to fabricate Li-incorporated titanium oxide, which is one of the successes of LTO. Hereafter, we refer to the obtained nanostructured titanium oxide as Li-TiO_x.

Figure 7 shows the TEM-EDS results. The presence of oxygen and titanium was confirmed in the nanostructured

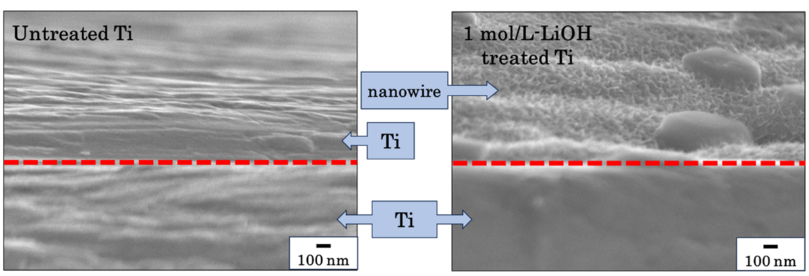

Figure 3. Edge of the SEM image of an untreated Ti(R) sample and a Ti sample treated with a 1 mol/L LiOH solution (L).

https://doi.org/10.1021/acsomega.4c04660
ACS Omega 2025, 10, 207−214

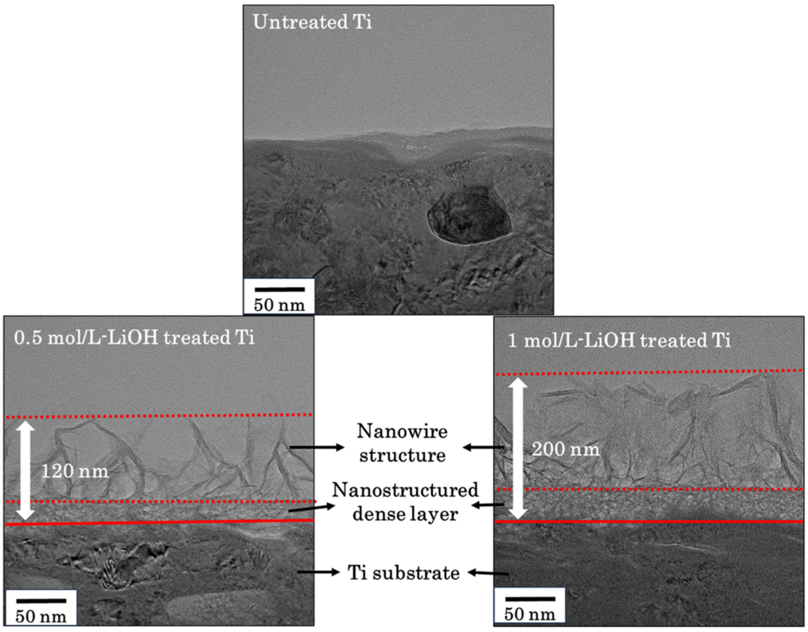

Figure 4. Cross-sectional TEM image of the untreated, 0.5, and 1 mol/L LiOH solution-treated Ti samples.

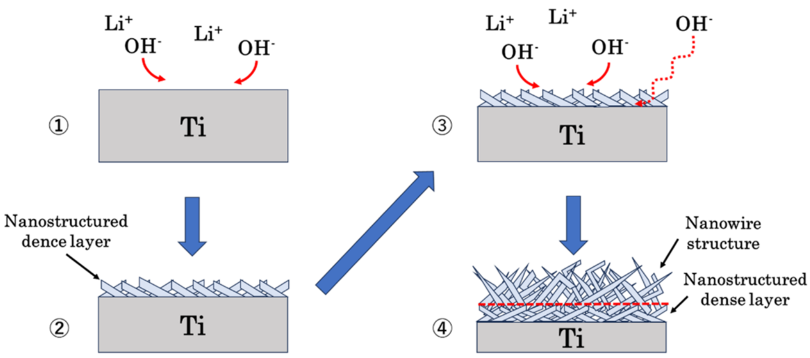

Figure 5. Schematic of nanowires growing mechanism. ① The Ti substrate is corroded by the LiOH solution. ② Titanium oxide forms as a dense layer. ③ The dense layer formed underwent further corrosion. At this stage, the dense layer was more susceptible to corrosion than the Ti substrate, resulting in the growth of nanowires. ④ A dense layer was formed near the less-corroded Ti substrate with nanowires forming on top of the dense layer, ultimately resulting in the formation of nanostructured titanium oxide.

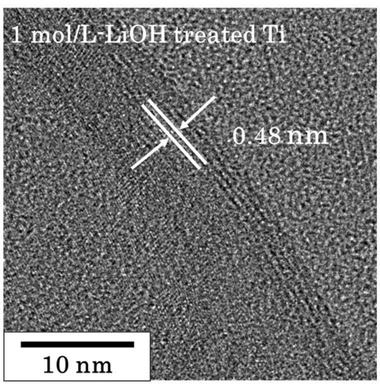

Figure 6. TEM images of nanostructured titanium oxide fabricated by using a 1 mol/L LiOH solution.

regions of the samples fabricated using 0.5 and 1 mol/L LiOH solutions. Therefore, it was confirmed that the fabricated nanostructures are titanium oxide.

The elemental composition of the nanostructured regions fabricated using 0.5 and 1 mol/L LiOH solutions is shown in Table 1.

3.3. AFM Observations to Verify the 3D Structure. Figure 8 illustrates the morphologies of the Ti substrate after WCP using AFM.

The three-dimensional (3D) surface images of the AFM show that the surface of the untreated Ti exhibits a relatively planar structure, whereas the fabricated Li-TiO_x confirms a 3D structure influenced by the nanostructures. In addition, the surface structure did not depend on the LiOH solution concentration.

The results of the surface area measurements obtained by AFM for untreated Ti and Ti surfaces treated with 0.5, 1, and 2 mol/L LiOH solutions are shown in Figure 9.

The surface area of the fabricated nanostructured Li-TiO_x increased by approximately 100 times compared to that of the untreated Ti, confirming the effect of the nanostructures. Moreover, little difference was observed in the surface areas of Ti treated with 0.5, 1, and 2 mol/L LiOH solutions. This is believed to be because, as shown in Figure 8, no differences

https://doi.org/10.1021/acsomega.4c04660
ACS Omega 2025, 10, 207−214

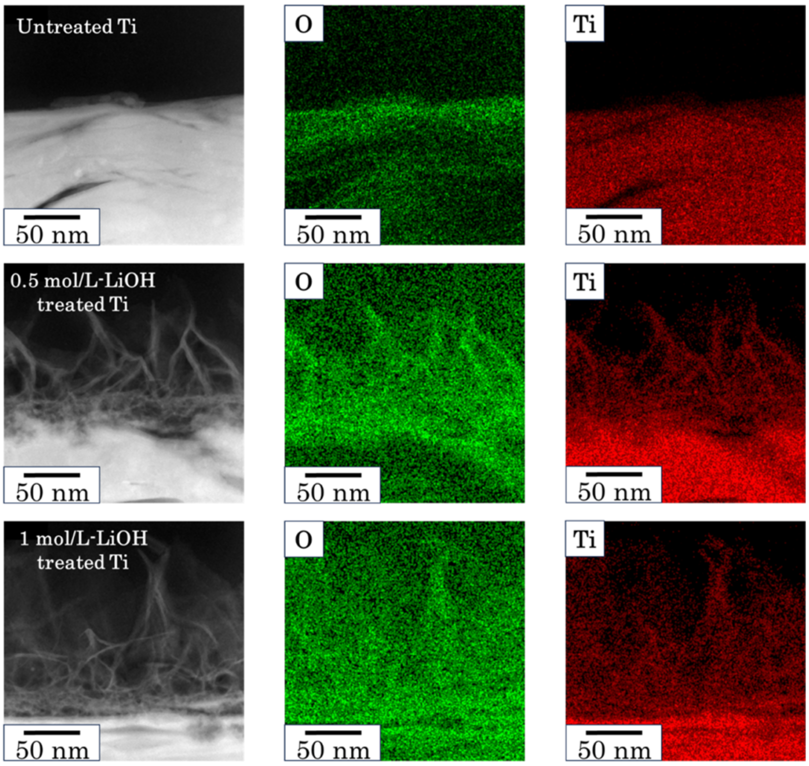

Figure 7. EDS via TEM image of untreated, 0.5, and 1 mol/L LiOH solution-treated Ti samples.

Table 1. Elemental Composition of the Samples Treated with 0.5 and 1 mol/L LiOH Solutions

	concentration of LiOH solution [mol/L]	
element [mass %]	0.5	1
Ti	18.41	17.6
O	81.59	82.4

were observed in the surface structure, regardless of the concentration used for the treatment.

3.4. Analysis of Elemental Composition and Chemical Bonding States by XPS. Figure 10 shows the XPS spectrum of the fabricated nanostructured Li-TiO_x using a 1 mol/L LiOH solution.

The peaks at 459.4 and 465.3 eV in the Ti 2p spectrum shown in Figure 10(a) corresponded to the binding energies of Ti^{4+} $2p_{1/2}$ and $2p_{3/2}$, respectively.[29] Therefore, it was determined that Ti exists in the Ti^{4+} oxidation state. Additionally, the peak at 531.0 eV in the O 1s spectrum shown in Figure 10(b) corresponds to the Ti−O bond. Therefore, the fabricated nanostructures were confirmed as titanium oxides.

Furthermore, the presence of peaks in the Li 1s spectrum (Figure 10c) indicated the presence of lithium within titanium oxide. Additionally, the peak at 63.0 eV in Figure 9(c) corresponds to the energy of the outermost electron orbitals of lithium, indicating the presence of Li^+ within the titanium oxide.[30]

Nanostructured Li-TiO_x, fabricated via WCP, is shown in Figure 11. This figure illustrates the potassium titanate structure, where K^+ ions are incorporated in the Ti−O layers. The structure was produced by treating the material with a KOH solution during WCP. In this study, because WCP treatment is conducted by using a LiOH solution, it is expected that a lithium titanate structure with Li^+ incorporated between the Ti−O layers can be fabricated. The presence of Li^+ within the Ti−O layers is expected to enhance the electrical properties, suggesting potential applications of negative electrode materials in lithium-ion batteries.

3.5. Analysis of Electrical Characteristics by *I*−*V* Curves. Figure 12 shows the results of the $I-V$ curves measured using a Keithley 6221 current meter and a Keithley 2182 voltmeter. The equation for a straight line on the graph is as follows

$$V = IR$$

Therefore, the slope of the line represents the resistance. The slope of the line representing the electrical characteristics of the fabricated nanostructured Li-TiO_x was observed to be smaller compared to that of the untreated Ti. Lower resistance indicates better electrical properties. Therefore, the fabricated Li-TiO_x demonstrates excellent electrical properties, indicating its potential applications in batteries. Based on the XPS results, these electrical properties originated from the incorporated Li in the titanium oxide.

Results of SEM, TEM, AFM, and $I-V$ curve analyses determined that the optimal condition was treatment with a 1 mol/L LiOH solution. This is because while the shape, surface area, and electrical properties of the nanostructured Li-TiO_x produced with 0.5, 1, and 2 mol/L LiOH solutions show little variation, the thickness of the layers of nanostructures confirmed by TEM is significantly greater when using a 1 mol/L LiOH solution compared to a 0.5 mol/L LiOH solution. This suggests that the nanostructures were denser and could accommodate a larger number of Li^+ ions, leading to enhanced performance. Increasing the concentration of Li^+ in nanostructured Li-TiO_x is believed to enhance the Li^+

https://doi.org/10.1021/acsomega.4c04660
ACS Omega 2025, 10, 207−214

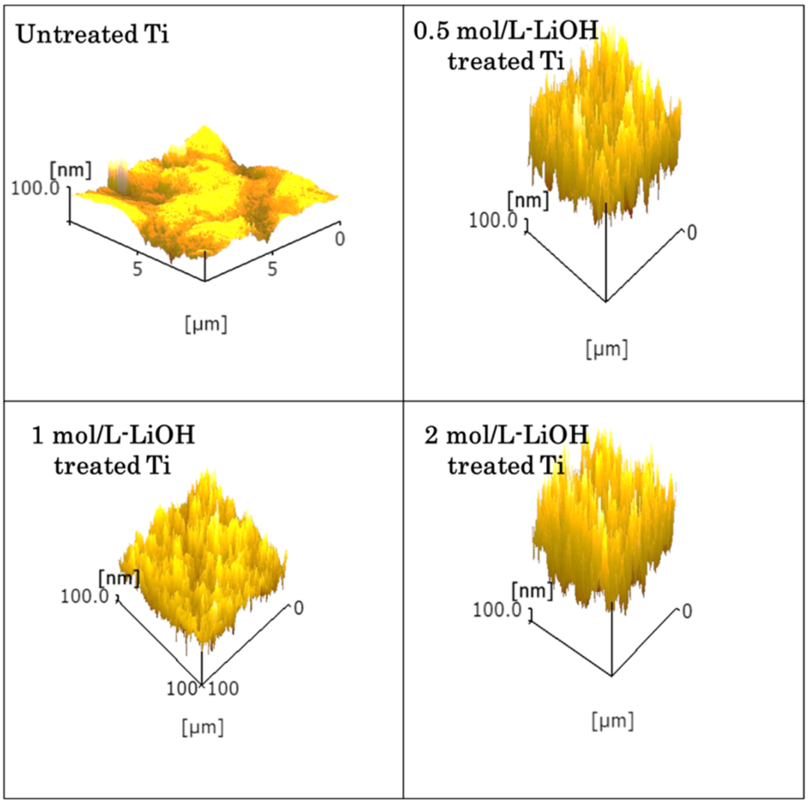

Figure 8. 3D morphologies of the surface of the untreated and 0.5, 1, and 2 mol/L LiOH solution-treated Ti samples.

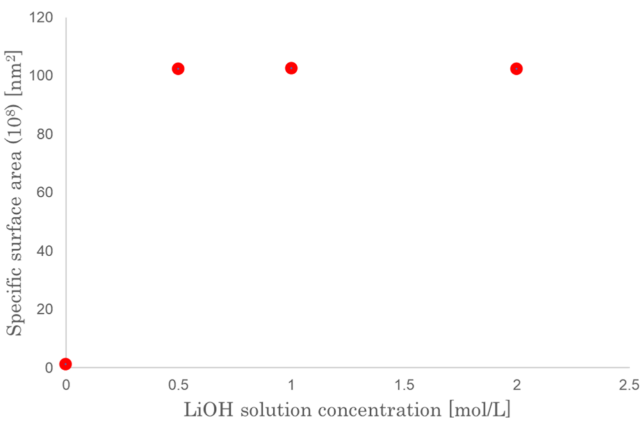

Figure 9. Specific surface area of untreated and 0.5, 1, and 2 mol/L LiOH solution-treated Ti samples.

deintercalation reaction, enabling a higher battery capacity and rapid charging capabilities.

4. CONCLUSIONS

In this study, we employed a WCP using a LiOH solution to fabricate nanostructured Li-TiO_x on Ti substrates. Additionally, we investigated the fabrication conditions and properties of the nanostructured Li-TiO_x. We also explored their potential applications in batteries.

The SEM results revealed that nanostructured Li-TiO_x could be fabricated within the concentration range of 0.5 to 2 mol/L of LiOH solution. Furthermore, TEM results confirmed that the fabricated nanostructures exhibited a wire-like morphology with diameters ranging from 5 to 10 nm. Additionally, the fabrication of nanostructures via WCP involves a mechanism in which the initial corrosion of the Ti substrate leads to the formation of a dense layer of titanium oxide, followed by further corrosion, which promotes the growth of nanowires. The thickness of the layer comprising the nanostructures, including the dense layer, was confirmed to be 120 nm when treated with a 0.5 mol/L LiOH solution and 200 nm when treated with a 1 mol/L LiOH solution. Therefore, 1 mol/L LiOH solution is considered to be the optimal condition.

The AFM results confirmed that the fabricated nanostructures exhibited an overall three-dimensional structure. Furthermore, compared with the untreated material, the specific surface area increased by approximately 100 times, indicating a significant enhancement owing to the nanostructure effect.

Based on the EDS and XPS results, it was determined that the fabricated nanostructures consisted of oxide. Additionally, analysis of the Li 1s XPS spectrum revealed the presence of Li^+ ions within the titanium oxide structure. Furthermore, the improvement in the electrical characteristics due to the incorporation of Li^+ ions into the fabricated nanostructured Li-TiO was confirmed by the *I*−*V* curve.

Based on the above result, WCP promises a brand new method to produce tunable nanostructures. And it can be concluded that a 1 mol/L LiOH solution is the optimal condition for fabricating nanostructured Li-TiO_x via WCP. Additionally, the fabricated nanostructured Li-TiO_x exhibited a significant increase in the specific surface area and an improvement in the electrical properties owing to the incorporation of Li^+ ions. These results are the first scientific report using WCP to provide Li-TiO_x for a battery, so it can be considered very worthwhile research. In brief, it is evident that nanostructured Li-TiO_x fabricated through WCP treatment using LiOH solution holds great promise for application as

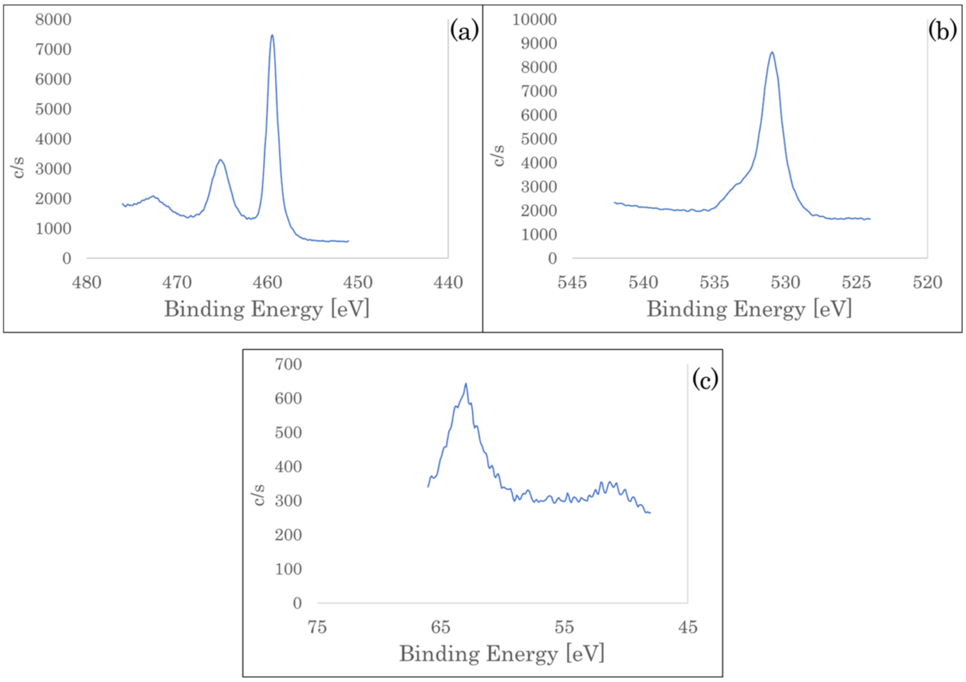

Figure 10. XPS spectra of (a) Ti 2p, (b) 1s, and (c) Li 1s.

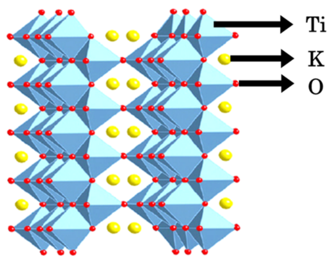

Figure 11. Structure of nanostructured titanium oxide obtained through WCP[31].

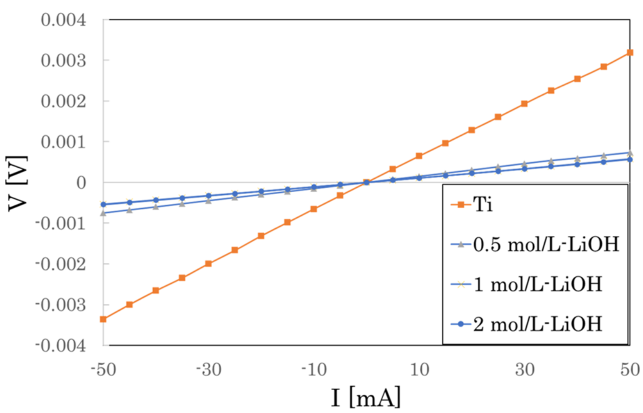

Figure 12. *I*−*V* curves of untreated Ti and Ti treated with LiOH solutions of 0.5, 1, and 2 mol/L concentrations.

negative electrode materials in next-generation batteries such as LTO batteries.

■ AUTHOR INFORMATION

Corresponding Author

So Yoon Lee − *Department of Materials Science and Engineering, College of Engineering, Shibaura Institute of Technology, Koto-ku, Tokyo 135-8548, Japan;* orcid.org/0000-0002-6786-356X; Phone: +81-3-5859-8776; Email: soyoon@shibaura-it.ac.jp

Authors

Hiroto Suzuki − *Department of Applied Chemistry, College of Engineering, Shibaura Institute of Technology, Koto-ku, Tokyo 135-8548, Japan*

Takumi Nishiguchi − *Department of Applied Chemistry, College of Engineering, Shibaura Institute of Technology, Koto-ku, Tokyo 135-8548, Japan*

Yuta Igawa − *Graduate School of Engineering and Science, Shibaura Institute of Technology, Koto-ku, Tokyo 135-8548, Japan*

Hiroya Oshiumi − *Graduate School of Engineering and Science, Shibaura Institute of Technology, Koto-ku, Tokyo 135-8548, Japan*

Ki-Young Lee − *Center for Spintronics, Korea Institute of Science and Technology, Seoul 02792, Korea;* orcid.org/0000-0002-9327-2026

Sanghoon Kim − *Department of Physics, University of Ulsan, Ulsan 44610, Korea*

Eunji Im − *Department of Physics, University of Ulsan, Ulsan 44610, Korea*

Siha Lee − *Department of Physics, University of Ulsan, Ulsan 44610, Korea;* orcid.org/0009-0007-7799-7952

Haneul Kim − *Department of Physics, University of Ulsan, Ulsan 44610, Korea*

Hatsuko Yoshikubo − *Innovative Global Program, College of Engineering, Shibaura Institute of Technology, Koto-ku, Tokyo 135-8548, Japan*

Hazime Kiyono − *Department of Applied Chemistry, College of Engineering, Shibaura Institute of Technology, Koto-ku, Tokyo 135-8548, Japan*

Complete contact information is available at: https://pubs.acs.org/10.1021/acsomega.4c04660

https://doi.org/10.1021/acsomega.4c04660
ACS Omega 2025, 10, 207−214

Notes

The authors declare no competing financial interest.

■ ACKNOWLEDGMENTS

This research(work) was supported by Next-generation Intelligence semiconductor R&D Program through the National Research Foundation of Korea (NRF) funded by the Korea government (MSIT) (RS-2023-00215802)

■ REFERENCES

(1) Weller, M.; Overton, T.; Rourke, J.; Armstrong, F. *Schreiber-Atkins Inorganic Chemistry (Lower)*, 6th ed.; Tokyo Kagaku Dozin: Tokyo, 2017; p 829.

(2) Yonezawa, T.; Asakura, K.; Ikuhara, Y. *Practical Aspects of Nanomaterials Analysis*; Kodansha: Tokyo, 2016; p 1.

(3) Jeevanandam, J.; Barhoum, A.; Chan, Y. S.; Dufresne, A.; Danquah, M. K. Review on nanoparticles and nanostructured materials: history, sources, toxicity and regulations. *Beilstein J. Nanotechnol.* **2018**, *9*, 1050−1074.

(4) Noah, N. M. Design and Synthesis of Nanostructured Materials for Sensor Applications. *J. Nanomater.* **2020**, *2020*, No. 8855321.

(5) Hirao, K. *Nanostructured Materials Engineering System, New Ceramics and Glasses*; Fuji Techno System: Tokyo, 2005; Vol. *1*, pp 5−10.

(6) Hashimoto, K.; Irie, H.; Fujishima, A. TiO_2 Photocatalysis: A Historical Overview and Future Prospects. *Jpn. J. Appl. Phys.* **2005**, *44*, No. 8269.

(7) Haghighi, F. H.; Mercurio, M.; Cerra, S.; Salamone, T.; Bianymotlagh, R.; Palocci, C.; Spica, V.; Fratoddi, I. Surface modification of TiO_2 nanoparticles with organic molecules and their biological applications. *J. Mater. Chem. B* **2023**, *11*, 2334−2366.

(8) Jafari, S.; Mahyad, B.; Hashemzadeh, H.; Janfaza, S.; Gholikhani, T.; Tayebi, L. Biomedical Applications of TiO_2 Nanostructures: Recent Advances. *Int. J. Nanomed.* **2020**, *15*, 3447−3470.

(9) Nasrollahzadeh, M.; Issaabadi, Z.; Sajjadi, M.; Sajadi, S. M.; Atarod, M. Types of Nanostructures. In *Interface Science and Technology*; Elsevier, 2019; pp 29−80.

(10) Lee, S. Y.; Lee, C. H.; Kim, D. Y.; Locquet, J. P.; Seo, J. W. Preparation and Photocatalytic Activity of Potassium-Incorporated Titanium Oxide Nanostructures Produced by the Wet Corrosion Process Using Various Titanium Alloys. *Nanomaterials* **2015**, *5*, 1397−1417.

(11) Guilbault, G. G.; Kramer, D. N.; Cannon, P. L. Electrochemical determination of organophosphorus compounds. *Anal. Chem.* **1962**, *34*, 1437−1439.

(12) Palecek, E. Past, present and future of nucleic acids electrochemistry. *Talanta* **2002**, *56*, 809−819.

(13) Horváth, E.; Kukovecz, A.; Konya, Z.; Kiricsi, I. Hydrothermal conversion of self-assembled titanate nanotubes into nanowires in a revolving autoclave. *Chem. Mater.* **2007**, *19*, 927−931.

(14) Wang, B. L.; Chen, Q.; Hu, J.; Li, H.; Hu, Y. F.; Peng, L.-M. Synthesis and characterization of large scale potassium titanate nanowires with good Li-intercalation performance. *Chem. Phys. Lett.* **2005**, *406*, 95−100.

(15) Bavykin, D. V.; Carravetta, M.; Kulak, A. N.; Walsh, F. C. Application of magic-angle spinning NMR to examine the nature of protons in titanate nanotubes. *Chem. Mater.* **2010**, *22*, 2458−2463.

(16) Lee, S. Y.; Matsuno, R.; Ishihara, K.; Takai, M. Electrical transport ability of nanostructured potassium-doped titanium oxide film. *Appl. Phys. Express* **2011**, *4*, No. 025803.

(17) Serrapede, M.; Savino, U.; Castellino, M.; Amici, J.; Bodoardo, S.; Tresso, E.; Chiodoni, A. Li+ Insertion in Nanostructured TiO_2 for Energy Storage. *Materials* **2020**, *13*, No. 21.

(18) Malati, M. A.; Wong, W. K. Doping TiO_2 for solar energy applications. *Surf. Technol.* **1984**, *22*, 305−322.

(19) Wong, W. K.; Malati, M. A. Doped TiO_2 for solar energy applications. *Sol. Energy* **1986**, *36*, 163−168.

(20) Raphael, M. W.; Malati, M. A. The photocatalysed reduction of aqueous sodium carbonate using platinized titania. *J. Photochem. Photobiol., A* **1989**, *46*, 367−377.

(21) Kudo, A.; Kondo, T. Photoluminescent and photocatalytic properties of layered caesium titanates, $Cs_2Ti_nO_{2n+1}$ (n = 2,5,6). *J. Mater. Chem.* **1997**, *7*, 777−780.

(22) Shibata, M.; Kudo, A.; Tanaka, A.; Domen, K.; Maruya, K.; Onishi, T. Photocatalytic activities of layered titanium compounds and their derivatives for H_2 evolution from aqueous methanol solution. *Chem. Lett.* **1987**, *16*, 1017−1018.

(23) Sato, T.; Yamamoto, Y.; Fujishiro, Y.; Uchida, S. Intercalation of iron oxide in layered $H_2Ti_4O_9$ and $H_4Nb_6O_{17}$: Visible-light induced photocatalytic properties. *J. Chem. Soc., Faraday Trans.* **1996**, *92*, 5089−5092.

(24) Fujishima, A.; Honda, K. Electrochemical photolysis of water at a semiconductor electrode. *Nature* **1972**, *238*, 37−38.

(25) Hoyer, P. Semiconductor nanotube formation by a two-step template process. *Adv. Mater.* **1996**, *8*, 857−859.

(26) Lakshmi, B. B.; Patrissi, C. J.; Martin, C. R. Sol-gel template synthesis of semiconductor oxide micro- and nanostructures. *Chem. Mater.* **1997**, *9*, 2544−2550.

(27) Yuan, Z. Y.; Zhou, W.; Su, B. L. Hierarchical interlinked structure of titanium oxide nanofibers. *Chem. Commun.* **2002**, *11*, 1202−1203.

(28) Masaki, N.; Uchida, S.; Yamane, H.; Sato, T. Hydrothermal synthesis of potassium titanates in Ti-KOH-H_2O system. *J. Mater. Sci.* **2000**, *35*, 3307−3311.

(29) Xu, H.; Chen, J.; Li, Y.; Guo, X.; Shen, Y.; Wang, D.; Zhang, Y.; Wang, Z. Fabrication of $Li_4Ti_5O_{12}$-TiO_2 Nanosheets with Structural Defects as High-Rate and Long-Life Anodes for Lithium-Ion Batteries. *Sci. Rep.* **2017**, *7*, No. 2960.

(30) Mosa, J.; Vélez, J. F.; Reinosa, J. J.; Aparicio, M.; Yamaguchi, A.; Tadanaga, K.; Tatsumisago, M. $Li_4Ti_5O_{12}$ thin-film electrodes by sol−gel for lithium-ion microbatteries. *J. Power Sources* **2013**, *244*, 482−487.

(31) Nafeaa, I. A.; Zekry, A. F.; Khalifa, M. G.; Farag, A. B. F.; El-Hussiny, N. A.; El Hossiny, K.; Shalabi, M. E.-M. H. Sodium Titanates Formation by Roasting of Pellets or Powder Mixture of Soda Ash and Rossetta Region Ilmenite Ore Concentrate in Air. *Open J. Met.* **2014**, *04* (2), 29−39.

https://doi.org/10.1021/acsomega.4c04660
ACS Omega 2025, 10, 207−214